SLAC-PUB-8882
June 2001

DESIGN STUDIES OF POSITRON COLLECTION FOR THE NLC

Yuri K. Batygin, Vinod K. Bharadwaj, David C. Schultz, John C. Sheppard

Stanford Linear Accelerator Center, Stanford University, Stanford, CA 94309

Abstract

The positron source for the NLC project utilizes a 6.2 GeV electron beam interacting in a high-Z positron production target. The electromagnetic shower in the target results in large energy deposition which can cause damage to the target. Optimization of the collection system is required to insure long-term operation of the target with needed high positron yield into the 6-dimensional acceptance of the subsequent pre-damping ring. Positron tracking through the accelerating system indicates a dilution of the initial positron phase space density. Results of the studies on the development of the collector systems design are presented.

Presented at 2001 Particle Accelerator Conference, Chicago, Illinois, 18-22 June 2001

Work supported by the Department of Energy contract DE-AC03-76SF00515

DESIGN STUDIES OF POSITRON COLLECTION FOR THE NLC*

Yuri K. Batygin, Vinod K. Bharadwaj, David C. Schultz, John C. Sheppard
Stanford Linear Accelerator Center, Stanford University, Stanford, CA 94309, USA

Abstract

The positron source for the NLC project utilizes a 6.2 GeV electron beam interacting in a high-Z positron production target. The electromagnetic shower in the target results in large energy deposition which can cause damage to the target. Optimization of the collection system is required to insure long-term operation of the target with needed high positron yield into the 6-dimensional acceptance of the subsequent pre-damping ring. Positron tracking through the accelerating system indicates a dilution of the initial positron phase space density. Results of the studies on the development of the collector systems design are presented.

1 INTRODUCTION

The positron injector includes a production target followed by a short solenoid with a strong magnetic field (flux concentrator), a 250 MeV linac with 0.5 Tesla focusing solenoids, a 1.73 GeV linac with quadrupole focusing, and an energy compressor system before injection into the positron pre-damping ring (PPDR). The preliminary design of injector is presented in Ref. [1], [2], [3]. The new set of parameters is listed in Tables 1, 2. The main changes in the requirements to the injector are imposed by a new value of PPDR normalized transverse acceptance of 0.045 π m rad instead of the previous value of 0.09 π m rad. The ultimate goal of the collector system is to provide the highest number of positrons within the 6-dimensional acceptance of the pre-damping ring.

2 POSITRON YIELD

As positron capture is restricted by the acceptance of the pre-dumping ring, it is convenient to select an energy-invariant 6-dimensional phase space volume and observe the dilution of positron phase space density inside this volume. The 6-dimensional volume is defined in canonical conjugate variables (x, P_x), (y, P_y), $(z - z_s, p - p_s)$, where P_x and P_y are the canonical momentum

$$P_x = p_x - \frac{e B_z}{2} y, \qquad P_y = p_y + \frac{e B_z}{2} x, \qquad (1)$$

p_x, p_y are the mechanical momentum, B_z is a longitudinal magnetic field, and z_s, p_s define the dynamics of synchronous particles. To insure proper capture of positrons into PPDR, the edge normalized emittance of the positron beam is selected to be ε_x, $\varepsilon_y \leq 0.03$ π m rad, bunch length σ_z = 6.97 mm and energy spread $\Delta E/E$ = 2% at the PPDR injection energy of E = 1.98 GeV. The value of energy spread corresponds to momentum spread of the beam $\Delta(\beta\gamma) = 80$. The positron yield is defined as a ratio of positrons in a volume of phase space per incident electron at the target, $Y_{e^+} = N_{e^+}/N_{e^-}$.

Table 1. Parameters of the electron beam drive for the positron target.

Parameter	Value
Energy	6.2 GeV
Bunch spacing	1.4 / 2.8 ns
Bunch energy variation	1% FW
Single bunch energy spread	1 % FW
Normalized emittance	10^{-4} π m rad
Transverse size, σ_x	1.6 mm
Bunch length, σ_z	5 mm
Particles/Bunch	$1.2 / 2.4.10^{10}$
Train population uniformity	1 % FW
Bunch-to-Bunch Pop. Unif.	2 % rms
Number of Bunches	190 / 95
Repetition Rate	120 Hz
Beam Power	271 kW

Table 2. Positron beam parameters.

Parameter	Value
Energy	1.98 GeV
Bunch spacing	1.4/2.8 ns
Bunch energy variation	1% FW
Single bunch energy spread	2 % FW
Normalized emittance	0.03 π m rad
Bunch length, σ_z	10 mm
Particles/Bunch	$0.9/1.8{\cdot}10^{10}$
Train population uniformity	1 % FW
Bunch-to-Bunch Pop. Unif.	2 % rms
Number of Bunches	190/95
Repetition Rate	120 Hz
Beam Power	58 kW

3 BEAM DYNAMICS IN INJECTOR

The initial positron distribution was obtained via Monte-Carlo simulation of electron-positron pair production utilizing the code EGS [4]. The positron beam created by an electromagnetic shower in solid target

*Work supported by the Department of Energy contract DE-AC03-76SF00515

possesses large momentum spread. The typical value of transverse positron emittance after the interaction of the incident 6.2 GeV electron beam of $\sigma_{x,y}$ = 1.6 mm with a W-Re target of 4 radiation lengths (RL) is ε_o = 0.135 π m rad. The production target is in the field of a tapered solenoid with a maximum field of B_t = 1.2 Tesla. The presence of a magnetic field at the target does not significantly increase the normalized beam emittance:

$$\varepsilon = \sqrt{\varepsilon_o^2 + (\frac{e\, B_t\, R_t^2}{2\, m\, c})^2} \approx \varepsilon_o \,. \qquad (2)$$

The created beam enters the strong longitudinal magnetic field of a flux concentrator. The flux concentrator is a solenoid with sharp increase of magnetic field up to peak value of 5.8 Tesla at a distance of 5 mm from the target and an adiabatic decrease of the field over a distance of 15 cm [5]. The strong magnetic field at the target is required to confine the emitted positron beam with its large momentum spread.

The flux concentrator is followed by a 250 MeV linac with an effective accelerating gradient of 25 MeV/m and transverse focusing by a 0.5 Tesla solenoid field. The transverse acceptance of the linac with solenoid focusing is energy independent:

$$\alpha = \frac{eB_z}{2\, mc}\, a^2 = 0.06\ \pi \text{ m rad} \,. \qquad (3)$$

After acceleration to 250 MeV positrons are accelerated in a linac with quadrupole focusing and an accelerating gradient of 15 MeV/m.

Tables 3 and Fig. 1 show the results of the positron beam dynamics simulation in the injector. The positron yield within the 6D phase space volume drops from the value of 4.7 at the target to 0.76 at the end of the linac. One of the reasons for the dilution of the beam phase space density in the linac is the beam energy spread, which results in chromaticity-induced beam emittance growth. Calculations were done for two cases, using longitudinal focusing: for a linac with solenoidal focusing with B = 0.5 Tesla, and a linac with focusing by periodic permanent magnets (PPM). The field of the PPM was approximated by function $B_Z = B_o \sin(2\pi z/L)$, where B_o = 0.5 Tesla is the maximum field and L = 50 cm was chosen to be the period of the PPM structure. Particle tracking indicates that in the case of longitudinal focusing, the positron yield at the end of the linac is increased to Y_{e^+} = 1.15.

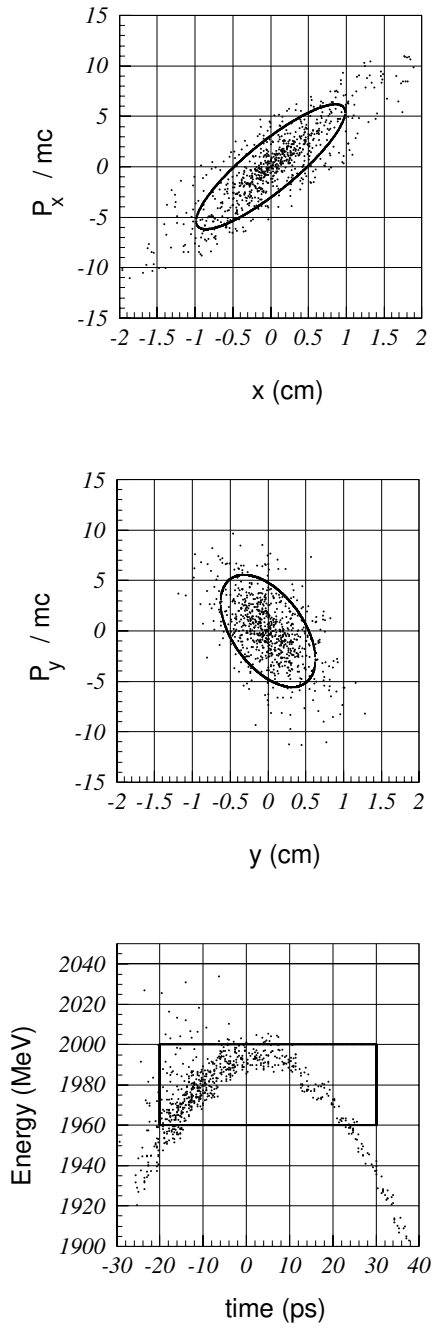

Fig. 1. Positron distribution at 1.98 GeV.

Table 3. Positron yield along the injector.

	After target	After flux concentrator	At 250 MeV	At 1.9 GeV
Positron yield	12	4.7	2.2	1.9
Fraction of positrons within 6-D phase space	0.39	0.37	0.74	0.40
Positron yield within 6-D phase space	4.70	1.76	1.60	0.76

4 DYNAMICS OF POLARIZED POSITRONS

One option for the positron injector being considered is the collection and acceleration of polarized positrons. Polarized positrons may be produced by targeting helically polarized gammas, which could be made by Compton backscattering [6] or with a helical undulator [7], on a thin target. To study the effects of positron depolarization, the particle tracking code was modified to include Thomas-BMT equation [8], describing the precession of the spin vector $\vec{S}$:

$$\frac{d\vec{S}}{dt} = \frac{e\,\vec{S}}{m\gamma} \times \left[(1+G\gamma)\vec{B}_{\perp}+(1+G)\vec{B}_{II}+(G\gamma + \frac{\gamma}{1+\gamma})\frac{\vec{E}\times\vec{\beta}}{c}\right], \quad (4)$$

where G is the anomalous magnetic moment of the positron, $\vec{E}$ is the electrical field, and $\vec{B}_{\perp}$ and $\vec{B}_{II}$ are components of the magnetic field perpendicular and parallel to the particle velocity. The spin advance at a small distance δz is described as a matrix [9] :

$$\begin{vmatrix} S_x \\ S_y \\ S_z \end{vmatrix} = \begin{vmatrix} 1- a(B^2+C^2) & ABa + Cb & ACa - Bb \\ ABa - Cb & 1- a(A^2+C^2) & BCa + Ab \\ ACa + Bb & BCa - Ab & 1- a(A^2+B^2) \end{vmatrix} \begin{vmatrix} S_{x,o} \\ S_{y,o} \\ S_{z,o} \end{vmatrix}, \quad (5)$$

$$A = \frac{D_x}{D_o},\ B = \frac{D_y}{D_o},\ C = \frac{D_z}{D_o},\ D_o = \sqrt{D_x^2 + D_y^2 + D_z^2}\ , \quad (6)$$

$$a = 1 - \cos(D_o\,\delta z)\ ,\ \ b = \sin(D_o\,\delta z)\ , \quad (7)$$

where components D_x, D_y, D_z are defined by the equations:

$$D_x = \frac{e}{m\,\gamma\,v}\left[(1+G\gamma)(B_x - x'B_z) + (1+G)x'B_z + \frac{v}{c^2}\left(\frac{\gamma}{1+\gamma} + G\gamma\right)(E_y - y'E_z)\right], \quad (8)$$

$$D_y = \frac{e}{m\gamma\,v}\left[(1+G\gamma)(B_y - y'B_z) + (1+G)y'B_z + \frac{v}{c^2}\left(\frac{\gamma}{1+\gamma} + G\gamma\right)(x'E_z - E_x)\right], \quad (9)$$

$$D_z = \frac{e}{m\,\gamma\,v}\left[(1+G\gamma)(-x'B_x - y'B_y) + (1+G)\cdot (x'B_x + B_z + y'B_y) + \frac{v}{c^2}\left(\frac{\gamma}{1+\gamma} + G\gamma\right)(y'E_x - E_y x')\right]. \quad (10)$$

Fig. 2 illustrates the polarization of positrons emerging from 0.2 RL W-Re target as a function of their energy, calculated by the EGS code extended to study polarization propagation in the target [10]. Polarization is defined as the probability to find the spin of the positron along the direction of the positron momentum.

During beam transport and acceleration, the spin vector precesses, resulting in the depolarization of the beam. We define the longitudinal polarization as an average of the product of the longitudinal component S_z and the value of polarization, P, over all positrons:

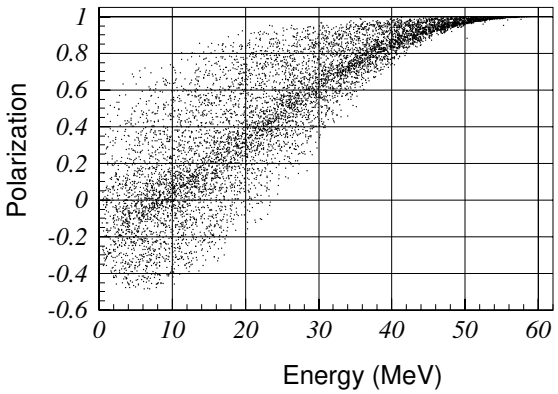

Fig. 2. Initial positron polarization from 60 MeV γ-rays.

Table 4. Polarization of positrons at 250 MeV captured within the 6-D phase space.

Energy range, MeV	Positron capture within 6D phase space	$\langle P_z \rangle$
260-280	0.028	0.92
255-280	0.038	0.86
245-280	0.084	0.68
242-280	0.11	0.60
240-280	0.14	0.53

$$\langle P_z \rangle = \frac{1}{N}\sum_{i=1}^{N} S_z^{(i)}\,P^{(i)}\ . \quad (11)$$

Table 4 illustrates the distribution of polarized positrons at 250 MeV. Simulation shows that 11% of the produced positrons have an average value of polarization of 60 %. Additional study is required to increase the number of captured positrons keeping the value of polarization high, and determine the needed γ - flux.

5 REFERENCES

[1] Zeroth-Order Design Report for the Next Linear Collider , SLAC-Report 474, (1996).

[2] T.Kotseroglou et. al., Proc. of the 1999 Particle Accelerator Conference, 3450 (1999).

[3] J.C. Sheppard et. al., "Update to the NLC Injector System Design", PAC 2001, June 2001.

[4] W.Nelson, H.Hirayama and D.Rogers, "The EGS4 Code System", SLAC-Report-265 (1985).

[5] A.V.Kulikov, S.D.Ecklund and E.M.Reuter, Proc. of the 1991 Particle Accelerator Conference, 2005 (1991).

[6] T.Omori, Proc. of the Workshop on New Kind of Positron Sources, Stanford, (1997), SLAC-R-502, p.285.

[7] A.Mikhailichenko, Proc. of the Workshop on New Kind of Positron Sources, Stanford, (1997), SLAC-R-502, p.229.

[8]V.Bargmann, L.Michel, V.L.Telegdi, Phys. Rev. Lett. 2 (1959) 435.

[9] Y.Batygin and T.Katayama, Physical Review E, Vol. 58, (1998), 1019.

[10] K.Flottmann, Ph.D. Thesis, DESY-93-161A (1993).